ESTIMATION OF LANDCOVER TYPES OVER HIMALAYAN REGION WITH THE CLASSIFICATION OF OPTICAL AND MICROWAVE-BASED IMAGE FUSION DATASET

S. Singh[1, *], R. K. Tiwari[2], V. Sood[3]

[1]Chitkara University School of Engineering and Technology, Chitkara University, Himachal Pradesh, India – sartajvir.singh@chitkaraunviersity.edu.in
[1,2,3] Indian Institute of Technology (IIT), Ropar, Punjab, India – reetkamal@iitrpr.ac.in
[3]Aiotronics Automation, Palampur, Himachal Pradesh, India – vishakha.sood@ieee.org

Commission III, WG III/6

KEYWORDS: Scatterometer Satellite (SCATSAT-1), Moderate Resolution Imaging Spectroradiometer (MODIS), Fusion, Classification algorithms.

ABSTRACT:

Himalayas play a significant role in terms of climate influence, the origin of rivers, hydropower generation, tourism, and forest wealth. The monitoring of the rugged terrain Himalayas via remote sensing is one of the efficient solutions to meet future requirements. In remote sensing, the sensors can be categorized as optical and microwave. The optical-based sensor provides multispectral or hyperspectral information at a very fine spatial resolution but is limited to daytime images without any penetration through the clouds. Whereas, the microwave works more effectively due to day/night image acquisition and cloud penetration capabilities. Therefore, the image fusion of multi-sensors (optical and microwave) datasets is important to extract crucial information about the Earth surface, especially over the Himalayas. However, the main aim of the article is to retrieve the different landcover types using various classifiers i.e., Linear Spectral Mixing (LSM), Random Forest Classifier (RFC), and Support Vector Machine (SVM) on the fused dataset. The dataset has been acquired over a part of Indian Himalayan terrain i.e., Uttarakhand State, India using microwave-based ISRO's Scatterometer Satellite (SCATSAT-1) and optical-based NASA's Moderate Resolution Imaging Spectroradiometer (MODIS). The results show the effectiveness of the RFC classifier in the mapping of land surface features as compared to other classification algorithms i.e., LSM and SVM. This study not only highlights the potential of the RFC classifier in the extraction of information but also, shows the significance of fusion of optical and microwave datasets in the extraction of important Earth surface features.

1. INTRODUCTION

The Himalayan region is one of the important sources of water for south Asian countries but due to the climate variability, the occurrence of flash floods and avalanches is also increased (Gurung et al., 2011). Remote sensing via spaceborne sensors plays an important role to provide the Earth surface imagery on daily basis. Therefore, the continuous monitoring of the Himalayas is essential to mitigate the impact of natural hazards (Ballesteros-Cánovas et al., 2018). Since past few decades, many improvements have been made in the spaceborne sensor in terms of spectral and spatial resolution to improve the pictorial representation and extract the crucial parameters from the Earth surface (Amro et al., 2011; Kahraman and Ertürk, 2017; Snehmani et al., 2017; Vivone et al., 2015).

The optical-based sensors acquire the Earth information in a huge range of wavelengths but are generally affected in the presence of differential illuminations and atmospheric conditions at a time of acquisitions (Rahman et al., 2010). Moreover, the optical sensors are not capable enough to penetrate through the clouds and thus, the applicability is limited (Tsai et al., 2019). On the other hand, microwave sensors depend on their source of illumination at microwave frequencies and thus, not much affected by differential illuminations and penetrate through the clouds (Ulaby and Long, 2015). Moreover, microwave-based sensors can also penetrate the surface to a certain extent depending upon the operating frequency and dielectric constant of the object (Shah et al., 2019). The microwave sensors provide useful information which may not be fetched from the multispectral or hyperspectral sensors but optical sensors are more competent in terms of reflective characteristics of the target (Rahman et al., 2010; Xiao et al., 2020).

Image fusion is a process of combining multiple images to improve visual perception and deliver more meaningful and suitable information for computer processing (Kulkarni and Rege, 2020). The fused dataset can be proven as useful in many scientific applications as crop yield estimation, forest cover mapping, management of natural resources and disaster management (Ghassemian, 2016). There are many optical and microwave sensors available with different technical features and characteristics. Here, we have considered Moderate Resolution Imaging Spectroradiometer (MODIS) as optical-based dataset and Scatterometer Satellite (SCATSAT-1) as microwave dataset because both datasets are freely available and provide the global imagery with more than 90% of coverage on daily basis. Moreover, many products are available for both datasets that can be utilized to enhance its applications ranges. In previous literature, different image fusion algorithms have been tested to fuse the optical and microwave imagery and nearest-neighbour based fusion (NNF) is found to be more accurate to compute the classified or change maps (Singh et al., 2021a). Therefore, the NNF approach has been utilized in the present work.

The classification of the fused dataset is one of the critical tasks in the accurate estimation of land use/cover type using the fused dataset. The classification algorithms are generally categorized into three categories based on their training procedure (Sood et al., 2018) such as (a) unsupervised that does not require inputs training sample from the user and deliver the outcomes based on similarity, (b) supervised that uses the labelled dataset to classify the datasets, (c) semi-supervised takes the middle ground and labels the unlabeled data points using knowledge learned from a limited number of labelled training samples (Lu and Weng, 2007; Myint et al., 2011).

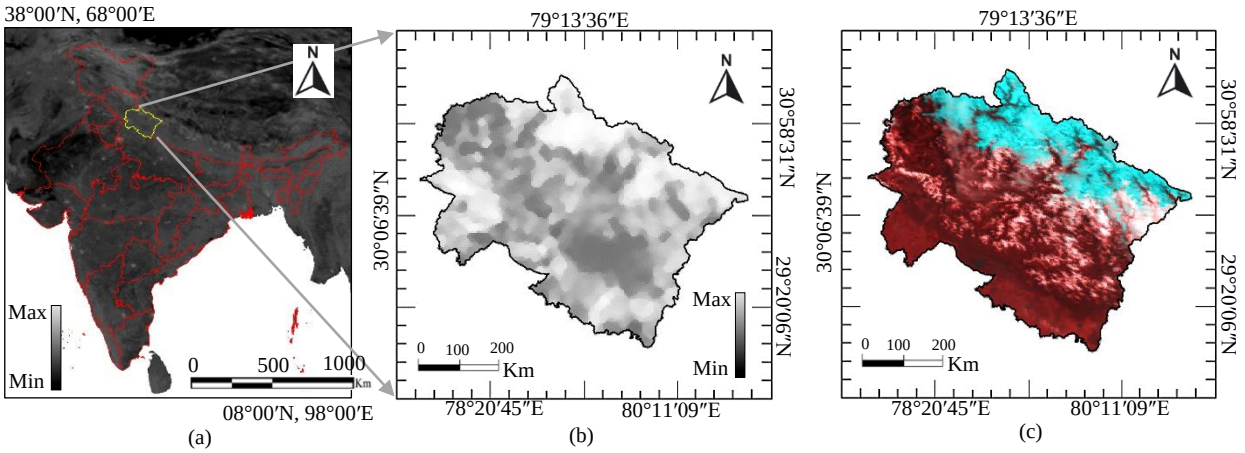

Fig. 1 Location of study site: (a) SCATSAT–1 image of India (highlighted area representing nominated study area); (b) SCATSAT–1 image (4–May–2020) of the study area (a part of Himalaya, India); (c) MODIS image (4–May–2020) of the study site.

The efficacy of any supervised classification algorithm is strongly dependent on the quality of samples used to train the classifier (Tuia et al., 2016). However, three well-defined supervised classifiers i.e., Linear Spectral Mixing (LSM) (Choodarathnakara et al., 2012; Du et al., 2014), Random Forest (RF) (Du et al., 2015; Shah et al., 2019), and Support Vector Machine (SVM) (Pal and Foody, 2012, 2010) have been evaluated in the present work to estimate the different landcover types over the Himalayas. In the present article, the main aim is to estimate the land-cover types using fusion datasets and evaluate the applicability of well-defined classification algorithms. To perform the image fusion for optical and microwave datasets, the NNF approach has been performed as previous studies confirmed the effectiveness of fusion of SCATSAT-1 and optical data (Singh et al., 2022a). Afterwards, different classification algorithms have been implemented such as LSM, RF and SVM. At last, the qualitative analysis has been performed to compute the effectiveness of each algorithm. The outcomes of the study allow the effective utilization of fused datasets in many applications.

2. STUDY AREA AND SATELLITE DATASETS

2.1 Study Area

The Indian State, Uttarakhand located in the north-western part of the country, has been selected to perform the methodology. It covers an area of about 55,483 sq. km lies between latitude 28°42′40″N to 31°27′43″N and longitude 77°35′02″E to 81°02′23″N as shown in Figure 1. The Uttarakhand lies within the Himalayas and is rich in natural resources such as the origin of many rivers, snow-clad mountain peaks, dense forests, and the exitance of many glaciers. Moreover, this state is also well known as Devbhumi (land of Gods) due to the existence of many Hindu pilgrimage's sites. This is one of the major reasons behind the attraction of tourism in the state.

On the other hand, it is more susceptible to high erosion, rainstorms, earthquakes, flash floods, avalanches, and glacial lake outburst flood (GLOF) (Gautam et al., 2013; Mool et al., 2001; Raza et al., 2012; You et al., 2017). This state is the witness of numerous natural hazards especially in the past decades due to the change in climate variability. Recently, flash floods were reported due to the collapse of a hanging glacier (Shugar et al., 2021). This natural disaster resulted in numerous deaths, property damage and also, impacted the hydropower plants. Therefore, it is essential to monitor the snow/ice cover changes in this region to forecast or mitigate the impact of natural hazards (Singh et al., 2021; Sood et al., 2020).

2.2 Satellite Dataset

There are two different datasets were utilized in this study i.e., ISRO's SCATSAT-1 as microwave data and NASA's MODIS as optical data. The SCATSAT-1 offers the daily-based backscattered coefficient (sigma-nought) at a frequency of 13.5 GHz in two different polarizations i.e., HH and VV. The SCATSAT-1 data is available in four-level of data products to enhance its applicability. On the other hand, the multispectral MODIS dataset offers information in 36 different spectral bands for different applications. However, we have utilized the first seven-band to merge with the microwave dataset. The band's details are shown in Table 1. The SCATSAT-1 and MODIS datasets were acquired on 4th May 2020 from the web-portals (https://www.mosdac.gov.in/) and (https://lpdaac.usgs.gov/), respectively. To validate the results, the 16-day MOD10A2 data product was acquired from a web portal (https://nsidc.org/) on the same period.

SCATSAT-1	**Specifications**	
Frequency	13.5 GHz	
Product Type	Level-4 (Sigma-nought)	
MODIS	**Band width**	**Applications**
Blue (B3)	459-479	Soil/Veg difference
Green (B4)	545-565	Green veg.
Red (B1)	620-670	Veg chlorophyll
NIR1 (B2)	841-876	Cloud/veg transformations
NIR2 (B5)	1230-1250	Leaf/canopy difference
SWIR1 (B6)	1628-1652	Snow/cloud difference
SWIR2 (B7)	2105-2155	Cloud/land properties

Table 1. Technical details of input bands.

3. METHODOLOGY

The methodology of the proposed work is shown in Figure 2. It is generally divided into four steps: (a) pre-processing, (b) image fusion, (c) classification, and (d) accuracy assessment.

3.1 Pre-processing

The SCATSAT-1 level 4 products involved the various types of corrections as explained in different studies (Mankad et al., 2019; Misra et al., 2019). The coded values are converted into dB according to equation (1).

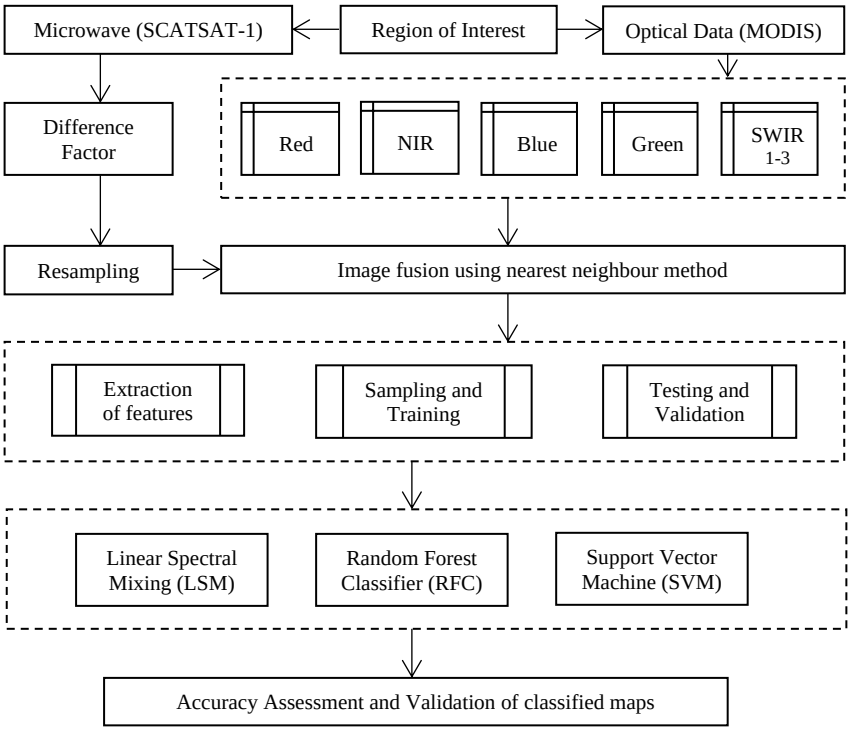

Fig. 2 Framework of methodology to combine the microwave and optical data, and perform the different classification algorithms and their accuracy assessment.

$$\sigma^0(dB) = (S \times DN) + O_v \quad (1)$$

Where S = slope of product parameters; σ^0 = image coordinates; O_v = offset value that normally considered as 0.001

3.2 Image fusion

To overcome the limitation of optical and microwave datasets and improve the extraction of land surface parameters, the image fusion approaches are very successful (Snehmani et al., 2017). Particularly, with the availability of optical and microwave datasets on daily basis at the global level (Kulkarni and Rege, 2020). They provide complementary information to deliver enhanced data products that can be utilized in numerous applications. Previous studies based on image fusion have been tested in numerous applications such as forest classification, land cover mapping, urban mapping and snow cover applications (Amro et al., 2011; Byun et al., 2015; Mishra and Susaki, 2014; Singh et al., 2020). The fusion of different sensors generally faces a problem of misalignment but scatterometers are sensitive towards the water contents within the snow which may helps in accurate detection of snow parameters (Singh et al., 2022b).

To perform the fusion on SCATSAT-1 and multispectral MODIS, the NNF approach has been followed. It is based on a nearest-neighbour approach that involved resampling, computation of the difference factor and linear mixing (Singh et al., 2021a; Sun et al., 2014). Here, both the datasets have been resampled at 500 m resolution and then, the difference factor is computed to estimate the similarity between low-resolution pixels and nearest-neighbour nine pixels. The value of the difference factor is calculated as a summation of the shortest geodesic distance that represents the difference of pixels in microwave data with respect to neighbour super-pixels in the optical dataset. It reconstructs the cloud containment pixels in the multispectral optical dataset (Singh et al., 2021b).

3.3 Classification

Classification is a standard procedure to generate thematic maps that correspond to the different class categories. Here, three different classifiers i.e., LSM, RFC and SVM have been implemented on the fused dataset. The LSM is a supervised classifier is one of the unique approaches to solve the mixed problem by assigning more than one class category to a particular pixel. It is very helpful to improve the outcomes of the coarse resolution datasets such as MODIS and SCATSAT-1. Whereas, the RFC as supervised is one of the widely used classification algorithms in solving many remote sensing problems. It comprises many trees and provides the means of averaging the prediction of various decision trees to avoid the problem of overfitting. It generally involves the selection of trees, optimum nodes, input spectral bands and exit criteria (Du et al., 2015; Pal, 2005). SVM is a supervised classifier that handles complex datasets to achieve better results (Vapnik, 2013). It involves structure-risk minimization to minimize the error rate in the training sampling procedure and improves the performance in the classification process as compared to other classification methods (Liu et al., 2018). On the other hand, support vectors also increase the complexity level of the algorithm. To compute the SVM, it is essential to select the various associated parameters such as degree polynomial, kernel function, threshold value and bias. The detailed information regarding the hyperspectral parameters and training dataset can be found in previous studies (Singh et al., 2022a; Sood et al., 2020a).

3.4 Accuracy Assessment

Accuracy assessment is essential to be applied on each thematic map to compute the efficacy of each algorithm. It plays a vital role in any classification project to compare the thematic image with the reference dataset. The major components include producer's accuracy (PA), user's accuracy (UA), overall accuracy (OA), and Kappa-coefficient (Kc).

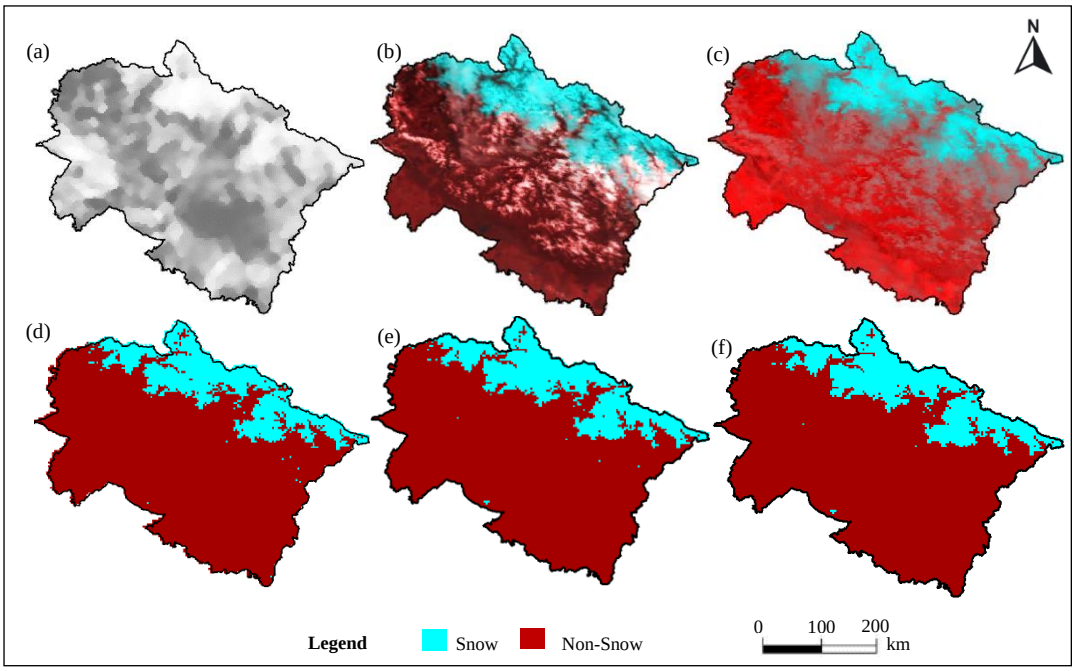

Fig. 3 Representation of (a) SCATSAT-1 image (sigma-nought), (b) MODIS imagery (RGB-611), (c) fused image, (d) Linear Spectral Missing (LSM), (e) Random Forest Classifier (RFC), and (f) Support Vector Machine (SVM).

4. RESULT ANALYSIS AND DISCUSSION

In the present work, two dairy-based datasets i.e., ISRO's SCATSAT-1 (microwave) and NASA's MODIS (optical) have been acquired on 4th May 2020 as shown in Figures 3(a) and 3(b), respectively. To integrate both datasets, the NNF-based fusion approach has been followed. It combines both optical and microwave datasets based on the nearest-neighbourhood method. The outcome of the NNF-based image fusion has been shown in Figure 3(c). It is noteworthy that microwave data can easily penetrate through the cloud whereas optical data is impacted in the presence of the clouds. But with the merging of both microwave and optical datasets, the impact of cloud has been reduced in the optical dataset which can be visualized in Figure 3(a)-(c).

Afterwards, three well-defined classifiers i.e., LSM, RFC and SVM have were implemented on the fused dataset. It is essential to check the performance of different classifier algorithms on fused datasets so that better outcomes can be attained. Figure 3 (d)-(f) has shown the comparison of thematic or classified maps generated via LSM, RFC and SVM classification algorithms. From the visual analysis, the outcomes are very close to each other. Therefore, the qualitative analysis (accuracy assessment) has also been computed as shown in Table 2. From the qualitative analysis, it has been observed that all the classifiers performed well enough (with OA of 93.99 – 94.15%).

But RFC performed marginally better (94.11 %) as compared to other classification algorithms i.e., LSM (94.11%) and SVM (93.99%). It has also been observed that in the snow category, the PA has been impacted in LSM (78.72%), RFC (88.871%) and SVM (80.59) which may be the reason behind such results.

The integration of SCATSAT-1 and MODIS dataset on a rugged terrain Himalayan region has a different degree of utilization as compared to other optical image fusion algorithms where the removal of cloud is a major concern. The image fusion and classification of fused dataset have an advantage in many remote sensing applications. It is expected that with the proposed work, many applications can be explored by merging the optical properties and scattering mechanisms of the object.

5. CONCLUSION

Based on the experimental outcomes, it is concluded that the image fusion of microwave-based SCATSAT-1 and optical-based MODIS offers better imagery as compared to the original images. This study has been evaluated the three classification algorithms on the fused dataset on a rugged terrain Himalayas region (Uttarakhand state, India). All the classification algorithms delivered satisfactory outcomes but RFC provided marginally better accuracy as compared to LSM and SVM. Future studies may incorporate the deep learning methods for the automatic extraction earth surface features.

	Snow					Non-Snow					Overall	
	RT	CT	NC	PA (%)	UA (%)	RT	CT	NC	PA (%)	UA (%)	OA (%)	Kc
LSM	3168	2559	2494	78.72	97.46	9808	10438	9744	99.35	93.35	94.11	0.83
RFC	3181	3014	2825	88.81	93.73	9785	9740	9400	96.07	96.51	94.15	0.8459
SVM	3168	2634	2553	80.59	96.92	9808	10216	9645	98.34	94.41	93.99	0.8321

Note: RT: Reference Total; CT: Classified Total; NC: Number of Correct; PA: Producer's Accuracy, UA: User's Accuracy, OA: Overall Accuracy, Kc: Kappa-coefficient

Table 2. Accuracy assessment of Linear Spectral Missing (LSM), Random Forest Classifier (RFC), and Support Vector Machine (SVM).

ACKNOWLEDGEMENT

The authors would like to express their gratitude to the anonymous referees and the editor for their constructive comments and valuable suggestions. Dr Sartajvir Singh wishes to thank the Science and Engineering Research Board (SERB) for research fellowship under the Teachers Associateship for Research Excellence (TARE) programme and Dr Vishakha Sood wishes to thank the Department of Science and Technology (DST), Govt. of India for research fellowship under the Women Scientist Scheme-A (WOS-A) programme. The authors would like to thank the Meteorological and Oceanographic Satellite Data Archival Centre (MOSDAC), Indian Space Research Organisation (ISRO) and Land Processes Distributed Active Archive Center (LP-DAAC) / National Snow and Ice Data Center (NSIDC), National Aeronautics and Space Administration (NASA) for providing the Scatterometer Satellite (SCATSAT-1) and Moderate Resolution Imaging Spectroradiometer (MODIS) data respectively for research purposes.

FUNDING

This research work is financially supported by Teachers Associateship for Research Excellence (TARE) Project (Grant no. TAR/2019/000354) by Science and Engineering Research Board (SERB), Govt. of India and Women Scientist Scheme-A (WOS-A) Project (Grant no. SR/WOS-A/ET-55/2019) by Department of Science and Technology (DST), Govt. of India.

REFERENCES

Amro, I., Mateos, J., Vega, M., Molina, R., Katsaggelos, A.K., 2011. A survey of classical methods and new trends in pansharpening of multispectral images. EURASIP J. Adv. Signal Process. 2011, 1–22. https://doi.org/10.1186/1687-6180-2011-79

Ballesteros-Cánovas, J.A., Trappmann, D., Madrigal-González, J., Eckert, N., Stoffel, M., 2018. Climate warming enhances snow avalanche risk in the Western Himalayas. Proc. Natl. Acad. Sci. 115, 3410–3415. https://doi.org/10.1073/pnas.1716913115

Byun, Y., Han, Y., Chae, T., 2015. Image fusion-based change detection for flood extent extraction using bi-temporal very high-resolution satellite images. Remote Sens. 7, 10347–10363. https://doi.org/10.3390/rs70810347

Choodarathnakara, A.L., Kumar, T.A., Koliwad, S., 2012. Mixed Pixels: A Challenge in Remote Sensing Data Classification for Improving Performance. Int. J. Adv. Res. Comput. Eng. Technol. 1, 2278–1323.

Du, P., Liu, S., Liu, P., Tan, K., Cheng, L., 2014. Sub-pixel change detection for urban land-cover analysis via multi-temporal remote sensing images. Geo-Spatial Inf. Sci. 17, 26–38. https://doi.org/10.1080/10095020.2014.889268

Du, P., Samat, A., Waske, B., Liu, S., Li, Z., 2015. Random Forest and Rotation Forest for fully polarized SAR image classification using polarimetric and spatial features. ISPRS J. Photogramm. Remote Sens. 105, 38–53. https://doi.org/10.1016/j.isprsjprs.2015.03.002

Gautam, M.R., Timilsina, G.R., Acharya, K., 2013. Climate change in the Himalayas: current State of Knowledge. Policy research working paper 6516.

Ghassemian, H., 2016. A review of remote sensing image fusion methods. Inf. Fusion 32, 75–89. https://doi.org/10.1016/j.inffus.2016.03.003

Gurung, D.R., Kulkarni, A. V., Giriraj, A., Aung, K.S., Shrestha, B., Srinivasan, J., 2011. Changes in seasonal snow cover in Hindu Kush-Himalayan region. Cryosph. Discuss. 5, 755–777. https://doi.org/10.5194/tcd-5-755-2011

Kahraman, S., Ertürk, A., 2017. A COMPREHENSIVE REVIEW of PANSHARPENING ALGORITHMS for GÖKTÜRK-2 SATELLITE IMAGES. ISPRS Ann. Photogramm. Remote Sens. Spat. Inf. Sci. 4, 263–270. https://doi.org/10.5194/isprs-annals-IV-4-W4-263-2017

Kulkarni, S.C., Rege, P.P., 2020. Pixel level fusion techniques for SAR and optical images: A review. Inf. Fusion 59, 13–29. https://doi.org/10.1016/j.inffus.2020.01.003

Liu, T., Abd-Elrahman, A., Morton, J., Wilhelm, V.L., 2018. Comparing fully convolutional networks, random forest, support vector machine, and patch-based deep convolutional neural networks for object-based wetland mapping using images from small unmanned aircraft system. GIScience Remote Sens. 55, 243–264. https://doi.org/10.1080/15481603.2018.1426091

Lu, D., Weng, Q., 2007. A survey of image classification methods and techniques for improving classification performance. Int. J. Remote Sens. 28, 823–870. https://doi.org/10.1080/01431160600746456

Mankad, D., Sikhakolli, R., Kakkar, P., Saquib, Q., Agrawal, K.M., Gurjar, S., Jain, D.K., Ramanujam, V.M., Thapliyal, P., 2019. SCATSAT-1 Scatterometer data processing. Curr. Sci. 117, 950–958. https://doi.org/10.18520/cs/v117/i6/950-958

Mishra, B., Susaki, J., 2014. SAR and optical data fusion for land use and cover change detection. Int. Geosci. Remote Sens. Symp. 4691–4694. https://doi.org/10.1109/IGARSS.2014.6947540

Misra, T., Chakraborty, P., Lad, C., Gupta, P., Rao, J., Upadhyay, G., Vinay Kumar, S., Saravana Kumar, B., Gangele, S., Sinha, S., Tolani, H., Vithani, V.K., Raman, B.S., Rao, C.V.N., Dave, D.B., Jyoti, R., Desai, N.M., 2019. SCATSAT-1 Scatterometer: An improved successor of OSCAT. Curr. Sci. 117, 941–949. https://doi.org/10.18520/cs/v117/i6/941-949

Mool, P.K., Wangda, D., Bajracharya, S.R., Kunzang, K., Gurung, D.R., Joshi, S.P., others, 2001. Inventory of glaciers, glacial lakes and glacial lake outburst floods. Monitoring and early warning systems in the Hindu Kush-Himalayan Region: Bhutan. Invent. glaciers, glacial lakes glacial lake outburst floods. Monit. early Warn. Syst. Hindu Kush-Himalayan Reg. Bhutan.

Myint, S.W., Gober, P., Brazel, A., Grossman-Clarke, S., Weng, Q., 2011. Per-pixel vs. object-based classification of urban land cover extraction using high spatial resolution imagery. Remote Sens. Environ. 115, 1145–1161. https://doi.org/10.1016/j.rse.2010.12.017

Pal, M., 2005. Random forest classifier for remote sensing classification. Int. J. Remote Sens. 26, 217–222. https://doi.org/10.1080/01431160412331269698

Pal, M., Foody, G.M., 2012. Evaluation of SVM, RVM and SMLR for accurate image classification with limited ground data. IEEE J. Sel. Top. Appl. Earth Obs. Remote Sens. 5, 1344–1355. https://doi.org/10.1109/JSTARS.2012.2215310

Pal, M., Foody, G.M., 2010. Feature selection for classification of hyperspectral data by SVM. IEEE Trans. Geosci. Remote Sens. 48, 2297–2307. https://doi.org/10.1109/TGRS.2009.2039484

Rahman, M.M., Sumantyo, J.T.S., Sadek, M.F., 2010. Microwave and optical image fusion for surface and sub-surface feature mapping in eastern Sahara. Int. J. Remote Sens. 31, 5465–5480. https://doi.org/10.1080/01431160903302999

Raza, I.U.R., Kazmi, S.S.A., Ali, S.S., Hussain, E., 2012. Comparison of Pixel-based and Object-based

classification for glacier change detection. Proc. 2nd Int. Work. Earth Obs. Remote Sens. Appl. EORSA 2012 259–262. https://doi.org/10.1109/EORSA.2012.6261178

Shah, E., Jayaprasad, P., James, M.E., 2019. Image Fusion of SAR and Optical Images for Identifying Antarctic Ice Features. J. Indian Soc. Remote Sens. 47, 2113–2127. https://doi.org/10.1007/s12524-019-01040-3

Shah, S.H., Angel, Y., Houborg, R., Ali, S., McCabe, M.F., 2019. A Random Forest Machine Learning Approach for the Retrieval of Leaf Chlorophyll Content in Wheat. Remote Sens. 11, 920. https://doi.org/10.3390/rs11080920

Shugar, D.H., Jacquemart, M., Shean, D., Bhushan, S., Upadhyay, K., Sattar, A., Schwanghart, W., McBride, S., de Vries, M.V.W., Mergili, M., Emmer, A., Deschamps-Berger, C., McDonnell, M., Bhambri, R., Allen, S., Berthier, E., Carrivick, J.L., Clague, J.J., Dokukin, M., Dunning, S.A., Frey, H., Gascoin, S., Haritashya, U.K., Huggel, C., Kääb, A., Kargel, J.S., Kavanaugh, J.L., Lacroix, P., Petley, D., Rupper, S., Azam, M.F., Cook, S.J., Dimri, A.P., Eriksson, M., Farinotti, D., Fiddes, J., Gnyawali, K.R., Harrison, S., Jha, M., Koppes, M., Kumar, A., Leinss, S., Majeed, U., Mal, S., Muhuri, A., Noetzli, J., Paul, F., Rashid, I., Sain, K., Steiner, J., Ugalde, F., Watson, C.S., Westoby, M.J., 2021. A massive rock and ice avalanche caused the 2021 disaster at Chamoli, Indian Himalaya. Science (80-.). 373, 300–306. https://doi.org/10.1126/science.abh4455

Singh, S., Sood, V., Prashar, S., Kaur, R., 2020. Response of topographic control on nearest-neighbor diffusion-based pan-sharpening using multispectral MODIS and AWiFS satellite dataset. Arab. J. Geosci. 13, 668. https://doi.org/10.1007/s12517-020-05686-z

Singh, S, Tiwari, R.K., Sood, V., Gusain, H.S., 2021. Detection and validation of spatiotemporal snow cover variability in the Himalayas using Ku-band (13.5 GHz) SCATSAT-1 data. Int. J. Remote Sens. 42, 805–815. https://doi.org/10.1080/2150704X.2020.1825866

Singh, S., Tiwari, R.K., Sood, V., Gusain, H.S., Prashar, S., 2022a. Image Fusion of Ku-Band-Based SCATSAT-1 and MODIS Data for Cloud-Free Change Detection Over Western Himalayas. IEEE Trans. Geosci. Remote Sens. 60, 1–14. https://doi.org/10.1109/TGRS.2021.3123392

Singh, S., Tiwari, R.K., Sood, V., Kaur, R., Prashar, S., 2022b. The Legacy of Scatterometers: Review of Applications and Perspective. IEEE Geosci. Remote Sens. Mag. 2–28. https://doi.org/10.1109/MGRS.2022.3145500

Singh, S., Tiwari, R.K., Sood, V., Prashar, S., 2021. Fusion of SCATSAT-1 and optical data for cloud-free imaging and its applications in classification. Arab. J. Geosci. 14, 1978. https://doi.org/10.1007/s12517-021-08359-7

Snehmani, Gore, A., Ganju, A., Kumar, S., Srivastava, P.K., Hari Ram, R.P., 2017. A comparative analysis of pansharpening techniques on quickbird and WorldView-3 images. Geocarto Int. 32, 1268–1284. https://doi.org/10.1080/10106049.2016.1206627

Sood, V., Gupta, S., Gusain, H.S., Singh, S., 2018. Spatial and Quantitative Comparison of Topographically Derived Different Classification Algorithms Using AWiFS Data over Himalayas, India. J. Indian Soc. Remote Sens. 46, 1991–2002. https://doi.org/10.1007/s12524-018-0861-4

Sood, V., Gusain, H.S., Gupta, S., Singh, S., Kaur, S., 2020a. Evaluation of SCATSAT-1 data for snow cover area mapping over a part of Western Himalayas. Adv. Sp. Res. 66, 2556–2567. https://doi.org/10.1016/j.asr.2020.08.017

Sood, V., Singh, S., Taloor, A.K., Prashar, S., Kaur, R., 2020b. Monitoring and mapping of snow cover variability using topographically derived NDSI model over north Indian Himalayas during the period 2008–19. Appl. Comput. Geosci. 100040. https://doi.org/10.1016/j.acags.2020.100040

Sun, W., Chen, B., Messinger, D.W., 2014. Nearest-neighbor diffusion-based pan-sharpening algorithm for spectral images. Opt. Eng. 53, 013107. https://doi.org/10.1117/1.oe.53.1.013107

Tsai, Y.-L.S., Dietz, A., Oppelt, N., Kuenzer, C., 2019. Remote Sensing of Snow Cover Using Spaceborne SAR: A Review. Remote Sens. 11, 1456. https://doi.org/10.3390/rs11121456

Tuia, D., Persello, C., Bruzzone, L., 2016. Domain Adaptation for the Classification of Remote Sensing Data: An Overview of Recent Advances. IEEE Geosci. Remote Sens. Mag. 4, 41–57. https://doi.org/10.1109/MGRS.2016.2548504

Ulaby, F., Long, D., 2015. Microwave radar and radiometric remote sensing. Artech House.

Vapnik, V., 2013. The nature of statistical learning theory. Springer science \& business media.

Vivone, G., Alparone, L., Chanussot, J., Mura, M.D., Garzelli, A., Member, S., Licciardi, G.A., Restaino, R., Wald, L., 2015. Pansharpening Algorithms 53, 2565–2586.

Xiao, X., Liang, S., He, T., Wu, D., Pei, C., Gong, J., 2020. Estimating fractional snow cover from passive microwave brightness temperature data using MODIS snow cover product over North America. Cryosph. Discuss. 1–40. https://doi.org/10.5194/tc-2019-280

You, Q.L., Ren, G.Y., Zhang, Y.Q., Ren, Y.Y., Sun, X.B., Zhan, Y.J., Shrestha, A.B., Krishnan, R., 2017. An overview of studies of observed climate change in the Hindu Kush Himalayan (HKH) region. Adv. Clim. Chang. Res. 8, 141–147. https://doi.org/10.1016/j.accre.2017.04.001